

Deformation mechanisms in an austenitic stainless steel (25Cr-20Ni) at elevated temperature

OSCAR A. RUANO

CENIM, Av. de Gregorio del Amo, s/n, Madrid 3, Spain

JEFFREY WADSWORTH

Metallurgy Department, Lockheed Palo Alto Research Laboratory, Palo Alto, California 94304, USA

OLEG D. SHERBY

Department of Materials Science and Engineering, Stanford University, Stanford, California 94305, USA

The creep behaviour at elevated temperature of an austenitic stainless steel (25Cr-20Ni), both with and without antimony additions, has been reanalysed. Formerly, the creep behaviour was interpreted by considering creep mechanisms based on diffusional (Coble) creep and threshold stresses. In the present paper, it is proposed that an alternative mechanism of grain boundary sliding, accommodated by slip in grain boundary mantle regions, can in fact be used to describe more accurately the creep behaviour. Quantitative predictions, based on phenomenological equations for describing creep controlled by grain boundary sliding, are made of the influences of grain size, stress and antimony addition on creep rates, and of the influence of grain size on the activation energy for creep of 25Cr-20Ni stainless steel. Comparison of these predictions with those based on creep models incorporating only diffusional flow are made. Furthermore, the existence of a threshold stress in creep of single-phase, massive materials is strongly questioned.

1. Introduction

Yamane and Takahashi and their colleagues [1-5] have thoroughly evaluated the influence of grain size, and antimony addition, on the steady-state creep rate of a 25Cr-20Ni stainless steel at high homologous temperatures, in the vicinity of $0.7T_m$. In a recent paper [5] the authors interpreted their results as follows: (a) an increase in grain size leads to a decrease in creep rate in the low- and intermediate-stress regimes but has no influence in the high stress regime; (b) a threshold stress for creep exists in the creep of the 25Cr-20Ni stainless steel in a creep regime they associate with diffusional (Coble) creep; and (c) antimony decreases the creep rate in the low-stress (diffusional creep) and intermediate-stress

(dislocation creep) regimes but has no influence in the high-stress regime.

It is the purpose of this paper to show that grain boundary sliding (gbs), a mechanism of plastic flow not considered by Yamane *et al.* [5], may in fact dominate deformation in the creep of fine-grained 25Cr-20Ni stainless steel. (Grain boundary sliding has been shown to be the principal deformation mechanism in fine-grained superplastic materials [6-11].) Introduction of gbs as a mechanism of deformation can explain quantitatively many of the observations noted by Yamane *et al.* [5] on the creep behaviour of 25Cr-20Ni stainless steel. It will be shown that the creep relation for gbs directly explains the effects of grain size and antimony on creep at

TABLE I The constitutive equations used for the construction of the deformation mechanism map shown in Fig. 1

Creep process	Equation	Reference
Diffusional flow		
Nabarro–Herring	$\dot{\epsilon} = 14 (D_L/d^2)(Eb^3/kT)(\sigma/E)$	[17, 18]
Coble	$\dot{\epsilon} = 50 (D_{gb}b/d^3/Eb^3/kT)(\sigma/E)$	[19]
Grain boundary sliding		
lattice diffusion controlled	$\dot{\epsilon} = 6.4 \times 10^9 (D_L/d^2)(\sigma/E)^2$	[20]
pipe diffusion controlled	$\dot{\epsilon} = 3.2 \times 10^{11} \alpha(D_p/d^2)(\sigma/E)^4$	[21]
grain boundary diffusion controlled	$\dot{\epsilon} = 5.6 \times 10^8 (D_{gb}b/d^3)(\sigma/E)^2$	[20]
Slip		
Harper–Dorn	$\dot{\epsilon} = 1.7 \times 10^{-11} (D_L/b^2)(Eb^3/kT)(\sigma/E)$	[22]
lattice diffusion controlled	$\dot{\epsilon} = 10^{11} (D_L/b^2)(\sigma/E)^5$	[23]
pipe diffusion controlled	$\dot{\epsilon} = 5 \times 10^{12} (D_p/b^2)(\sigma/E)^7$	[23]

The material constants used for construction of the deformation mechanism map at $0.7T_m$ are as follows: $E = 0.69 \times 10^5$ MPa, $b = 2.5 \times 10^{-10}$ m, $\alpha = 4$ (calculated from data of Fig. 2), $k = 1.38 \times 10^{-23}$ J K⁻¹, $T = 1173$ K, $D_{gb} = D_p = 9.8 \times 10^{-12}$ m² sec⁻¹, and $D_L = 1.68 \times 10^{-17}$ m² sec⁻¹.

low and intermediate stresses. Furthermore, it is predicted that no diffusional (Coble) creep will take place in the stress range studied, and no threshold stress for creep is expected in 25Cr–20Ni stainless steel.

2. Deformation mechanism map at $0.7T_m$

Equations are well established to describe the three principal mechanisms of plastic flow [12–16], namely, slip creep, grain boundary sliding and diffusional flow. Each of these mechanisms can be described by a constitutive equation of the form:

$$\dot{\epsilon} = A \left(\frac{b}{d} \right)^p \exp \left(- \frac{Q_c}{RT} \right) \left(\frac{\sigma}{E} \right)^n \quad (1)$$

where $\dot{\epsilon}$ is the steady-state creep rate; A , n and p are material constants, which have discrete values depending on the deformation mechanism; σ is the creep stress; E is the dynamic unrelaxed average Young's modulus; d is the grain size; b is Burgers' vector; R is the gas constant; T is the absolute temperature; and Q_c is the activation energy for plastic flow and is equal to either the activation energy for lattice diffusion (Q_L), the activation energy for dislocation pipe diffusion (Q_p), or the activation energy for grain boundary diffusion (Q_{gb}). For slip creep: $p = 0$, $n = 5$ when $Q_c = Q_L$; and $p = 0$, $n = 7$ when $Q_c = Q_p$. For grain boundary sliding: $n = 2$, $p = 2$ when $Q_c = Q_L$; $n = 2$, $p = 3$ when $Q_c = Q_{gb}$; and $n = 4$, $p = 2$ when $Q_c = Q_p$. For diffusional flow: $n = 1$,

$p = 2$ when $Q_c = Q_L$; and $n = 1$, $p = 3$ when $Q_c = Q_{gb}$.

A deformation mechanism map at $0.7T_m$ is constructed in Fig. 1 based on equations of the form given by Equation 1; a plot is made of the modulus-compensated flow stress as a function of grain size normalized by Burgers' vector. The constitutive equations used to prepare this map are given in Table I. The relations used to describe slip creep are those typical of close-packed metals with a high stacking fault energy. This figure illustrates the various mechanisms of plastic flow expected in a polycrystalline material as a function of modulus-compensated stress and grain size. The stress and grain size region covered by Yamane *et al.* [5] is shown in the figure. As can be seen, deformation of the 25Cr–20Ni stainless steel in this range is predicted to be principally by grain boundary sliding and by slip creep. Only if gbs is ignored as a mechanism does the diffusional creep regime become important. In the fine grain size range, e.g. $< 50 \mu\text{m}$, the map predicts up to five discrete regions that can be encountered with increasing σ/E . These are: diffusional flow governed by D_{gb} ($\dot{\epsilon} \propto \sigma$), gbs controlled by lattice diffusion (D_L) ($\dot{\epsilon} \propto \sigma^2$), gbs controlled by D_p ($\dot{\epsilon} \propto \sigma^4$), slip creep controlled by D_L ($\dot{\epsilon} \propto \sigma^5$) and slip creep controlled by D_p ($\dot{\epsilon} \propto \sigma^7$). From the viewpoint of a given intermediate stress, e.g. $\sigma \simeq 10^{-4}E$, the map predicts three discrete regions that are encountered with an increase in grain size: gbs controlled by D_{gb} , gbs controlled by D_p and slip creep controlled by D_L . Using a deformation

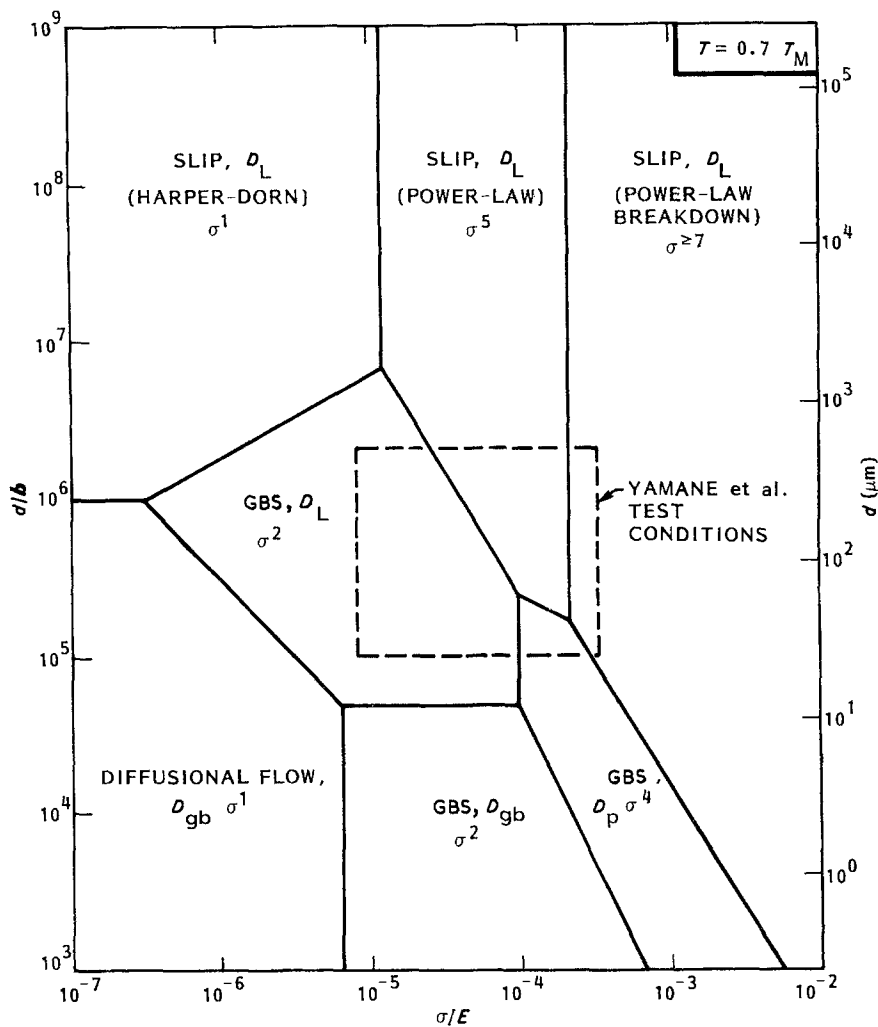


Figure 1 A deformation mechanism map for close-packed metals at $T = 0.7T_m$ is shown. The grain size and stress regimes used in the experimental study of Yamane *et al.* [5] on 25Cr-20Ni stainless steels are shown on the figure as the region bounded by broken lines.

map that includes the important contributions of gbs mechanisms, Coble creep is predicted not to occur in the stress range investigated by Yamane *et al.* and only becomes important at fine grain sizes and at values of σ/E below 3×10^{-6} .

It is predicted, in Fig. 1, that there is a large region for the mechanism of gbs controlled by D_L at $0.7T_m$. This area is one in which $\dot{\epsilon} \propto \sigma^2$ is expected to be observed. There is considerable evidence to support the existence of this wide region of creep behaviour from studies in fine-grained two-phase superplastic materials over the temperature range $0.65T_m$ to $0.85T_m$ [6, 7, 15, 24]. These studies have clearly shown that the creep rate of these materials is a power function

of the stress, where $n = 2$, and is an exponential function of the temperature where the activation energy for creep is that for lattice diffusion (Q_L). It is appropriate to use these results for comparison with the predominantly single-phase stainless steel investigated by Yamane *et al.* [5] because their creep studies were also conducted at a high homologous temperature ($0.7T_m$). In contrast, creep studies carried out on other stainless steels [25, 26] have been performed at a low homologous temperature ($0.55T_m$) where gbs controlled by D_L is not expected to control the creep rate; in this case gbs controlled by D_{gb} is expected [15, 21]. Thus analyses of the Yamane *et al.* data represent a first opportunity to establish whether or not D_L , as well as D_p ,

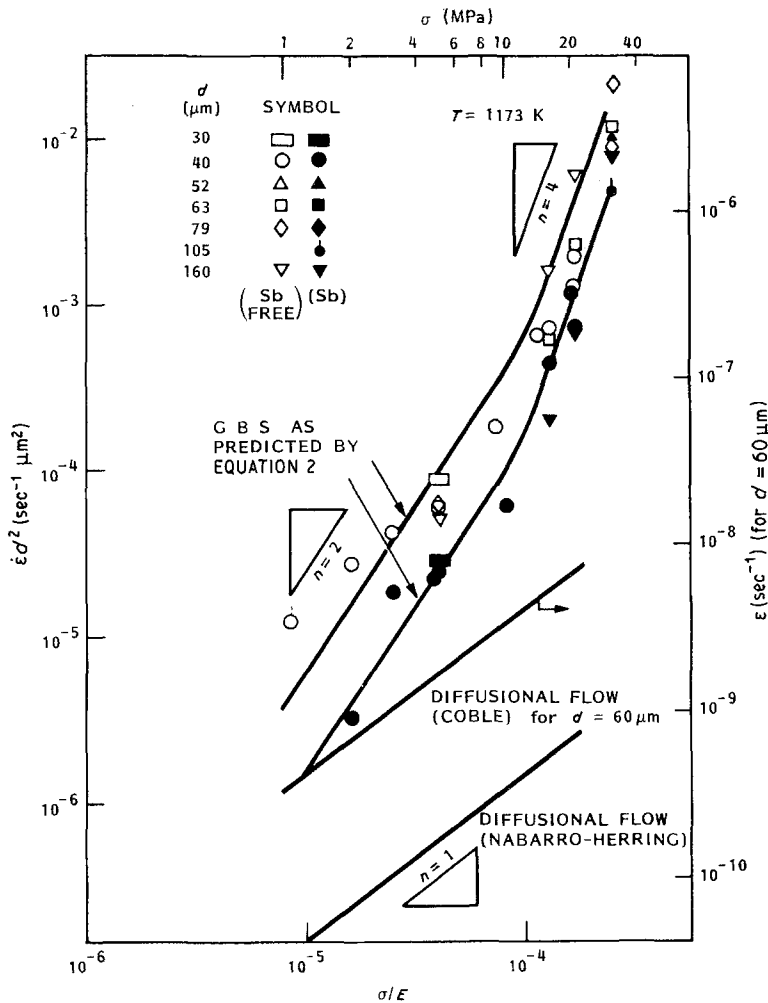


Figure 2 The predicted grain-size-compensated creep rate-modulus-compensated stress relations for both gbs and diffusional creep flow models are shown with experimental data for 25Cr-20Ni stainless steels from Yamane *et al.* [5].

controlled gbs creep mechanisms are important in describing the creep behaviour of a predominantly single-phase material.

3. Prediction of creep data on 25Cr-20Ni austenitic stainless steel

Yamane *et al.* [5] studied the influence of stress on the steady-state creep rate of 25Cr-20Ni austenitic stainless steel for a number of different grain sizes. Their data are plotted in Fig. 2 as grain-size-compensated strain rate, $\dot{\epsilon}d^2$, against the modulus-compensated stress. Both antimony-free and antimony-addition stainless steels are included in the graph. Predictions based on diffusional flow and on grain boundary sliding are given by the full lines shown in Fig. 2. The predicted lines from Nabarro-Herring creep and from Coble creep models are observed to result in creep rates that are considerably

below the experimental data. On the other hand, the predicted lines from the grain boundary sliding model show excellent agreement with the data. The constitutive equation for gbs used to predict the creep behaviour of the stainless steel is as follows [6, 7, 15, 24]:

$$\dot{\epsilon}_{\text{gbs}} = A \frac{D_{\text{eff}}}{d^2} \left(\frac{\sigma}{E} \right)^2 \quad (2)$$

Equation 2 is a phenomenological relation which is intended to describe grain boundary sliding in a mantle region at and adjacent to the grain boundary following the core-and-mantle model of Gifkins [11]. In this equation, $\dot{\epsilon}$ is the steady-state creep rate, d is the grain size, σ the creep stress, E the dynamic unrelaxed average Young's modulus, A is a material constant related to the structure of the grain boundary region ($\approx 10^9$), and D_{eff} is the effective diffusion

TABLE II Material constants and diffusion coefficients used for prediction of creep rates for 25Cr–20Ni stainless steel at $0.7T_m$ (1173 K)

Parameter	Antimony-free	Antimony-addition	Reference
A_{gbs}	4.0×10^9	9.0×10^8	this investigation
A_{slip}	8.6×10^8	8.6×10^8	this investigation
D_L ($\text{m}^2 \text{sec}^{-1}$)	1.68×10^{-17}	1.68×10^{-17}	[27]
Q_L (kJ m^{-1})	270	270	[27]
$(D_0)_L$ ($\text{m}^2 \text{sec}^{-1}$)	0.18×10^{-4}	0.18×10^{-4}	[27]
$D_p = D_{\text{gbs}}$ ($\text{m}^2 \text{sec}^{-1}$)	9.8×10^{-12}	9.8×10^{-12}	[28–30]
$Q_p = Q_{\text{gbs}}$ (kJ m^{-1})	163	163	[28–30]
$(D_0)_p = (D_0)_{\text{gbs}}$ ($\text{m}^2 \text{sec}^{-1}$)	1.8×10^{-4}	1.8×10^{-4}	[28–30]
E (MPa)	1.2×10^5	1.2×10^5	[31]
b (m)	2.58×10^{-10}	2.58×10^{-10}	–
α (for $\dot{\epsilon}_{\text{gbs}}$)	4.0	4.0	Fig. 2
f_p	$50 (\sigma/E)^2$	$50 (\sigma/E)^2$	[32]

coefficient defined as:

$$D_{\text{eff}} = (D_L + \alpha f_p D_p) \quad (3)$$

where D_L is the lattice diffusion coefficient, D_p the dislocation pipe diffusion coefficient, f_p the fraction of atoms associated with dislocations (assumed equal to about $50(\sigma/E)^2$) [23] and α is a constant. In order to fit the data of Yamane *et al.* [5] to Equation 2, the constant A was chosen as 4.0×10^9 and 9×10^8 for the antimony-free and antimony-addition stainless steels respectively, and α was made equal to 4. The specific values of the constants used for predictions with Equations 2 and 3 are given in Table II. The correlation shown in Fig. 2 is seen to be very good; discrete curves are shown for the two materials and they are displaced by an identical amount. The important feature of Fig. 2 is the transition from σ^2 to σ^4 behaviour in agreement with a change from gbs (D_L) to gbs (D_p) behaviour (as predicted from Fig. 1). The σ^4 prediction from Equation 2 arises from the contribution of the $\alpha f_p D_p$ term to creep at high stresses.

The data for the antimony-addition stainless steel shown in Fig. 2 are replotted in Fig. 3 to show the relation between grain size and the creep rate at stresses in the range over which both $\dot{\epsilon} \propto \sigma^2$ and $\dot{\epsilon} \propto \sigma^4$ behaviour is observed. The data relating $\dot{\epsilon}$ to d at various stresses are seen to be nearly parallel. This similar dependence of $\dot{\epsilon}$ on d would suggest the presence of a single deformation mechanism. The lines predicted using Equation 2 are also plotted in the figure and are seen to correlate quite well with the creep data. The relation between the creep rate and grain size, $\dot{\epsilon} \propto d^{-2}$, is confirmed by the

data; it is closely obeyed in the σ^2 range (the bottom line) as well as in the σ^4 range (the three top lines). Predictions made from the Coble relation are also shown. These predicted creep

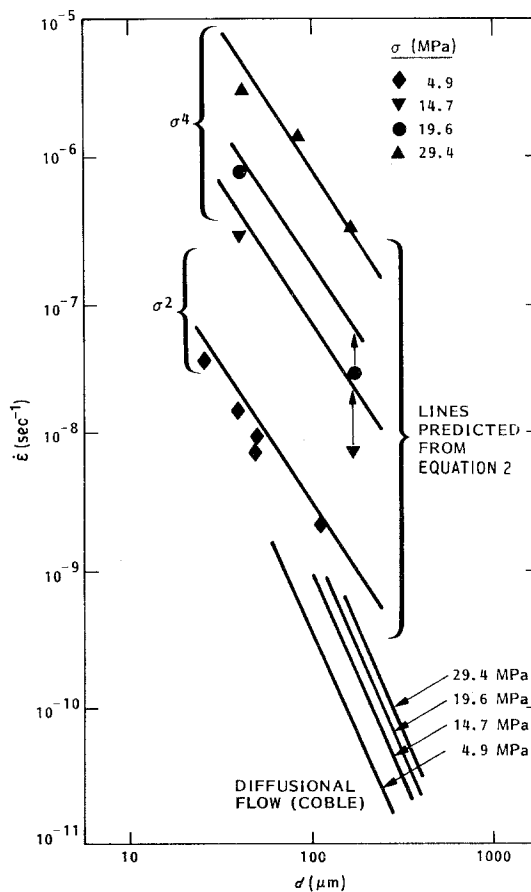


Figure 3 The influence of grain size on the creep rate at 1173 K is shown for the 25Cr–20Ni stainless steel over stress ranges in which $\dot{\epsilon} \propto \sigma^2$ and $\dot{\epsilon} \propto \sigma^4$ behaviour is observed. The individual data points are from the study of Yamane *et al.* [5] and the full lines are predictions from a gbs mechanism and from a diffusional (Coble) creep mechanism.

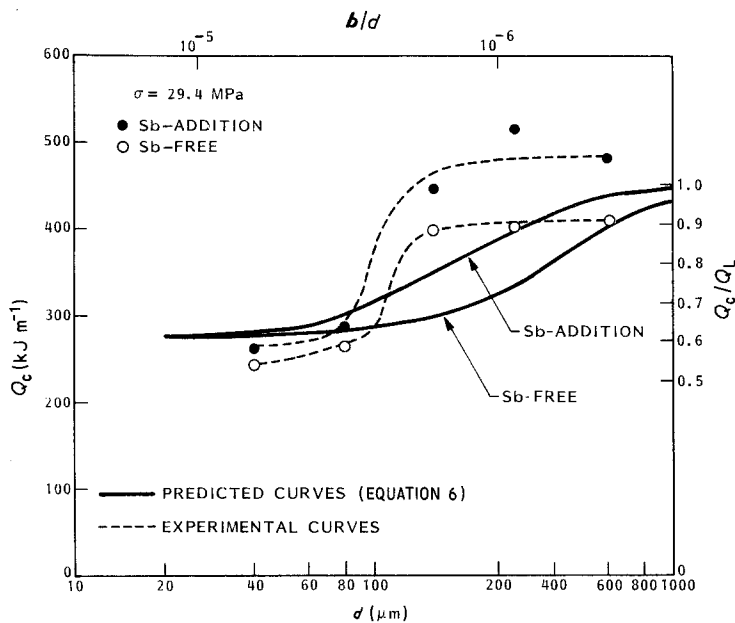


Figure 4 The influence of grain size on the activation energy for creep of 25Cr-20Ni steel. The predicted activation energy is plotted as a fraction of the lattice diffusion activation energy (Q_c/Q_L).

rates are considerably below the actual creep rates observed and the stress dependence, as shown by the displacement of curves, is seen to be altogether wrong. The good correlation of the creep data with Equation 2 shown in Fig. 3 is strong evidence for gbs as the dominating mechanism of plastic flow of 25Cr-20Ni steel in the grain size and stress range considered.

Yamane *et al.* [5] also investigated the influence of grain size on the activation energy for creep of the 25Cr-20Ni steels. Their data are shown in Fig. 4. As can be seen, the value of the activation energy increases from a low plateau value to a high plateau value with an increase in grain size. Yamane *et al.* attributed the change in activation energy to an internal stress effect which was considered to be a function of grain size. No quantitative explanation was given by the authors, however, for this observed trend. The deformation mechanism map of Fig. 1 provides a quantitative explanation. At high modulus-compensated stresses, e.g. $\sigma/E = 10^{-4}$, the rate-controlling process is seen to change with an increase in grain size. For fine grain sizes, gbs controlled by D_p dominates deformation, and for coarse grain sizes, slip creep controlled by D_L dominates deformation. This observation

predicts that the activation energy will increase with an increase in grain size, changing from Q_p at small grain size to Q_L at coarse grain size*. A quantitative prediction can be made by using the equation for D_p controlled gbs (Equation 2) and the equation for D_L controlled slip creep. The constants for the constitutive equations describing gbs creep and slip creep in 25Cr-20Ni steel are given in Table II. The pre-exponential constant for the slip creep equation, A_{slip} , was selected to fit the experimental data of Yamane *et al.* in the slip creep region. The constant, A_{slip} , was found to be equal to 8.6×10^8 in contrast to the value of 10^{11} used in preparing the deformation mechanism map given in Fig. 1. This is entirely consistent with the low value of A expected for a material of low stacking fault energy [16]. The stacking fault energy of 25Cr-20Ni stainless steel is low and equal to about 50 erg cm^{-2} (mJ m^{-2}) [34]. A single value of A_{slip} was chosen for the two 25Cr-20Ni stainless steels reflecting the reasonable assumption that the steady-state creep rate in this region is principally a function of the dislocation substructure (subgrain size) and is therefore independent of dilute antimony additions. Since the two processes of gbs and slip creep are independent, and therefore additive,

*The activation energies for creep obtained by Yamane *et al.* [5] are higher than the activation energy for creep involving Q_p (163 kJ mol^{-1}) and Q_L (270 kJ mol^{-1}). This difference has not been satisfactorily explained and is probably related to an additional temperature term which influences creep of stainless steels. Takahashi and Yamane [2] attribute the difference in activation energy to an "internal stress" effect, whereas, Schmidt and Miller [33] attribute the difference to a "solute atom-dislocation interaction" effect.

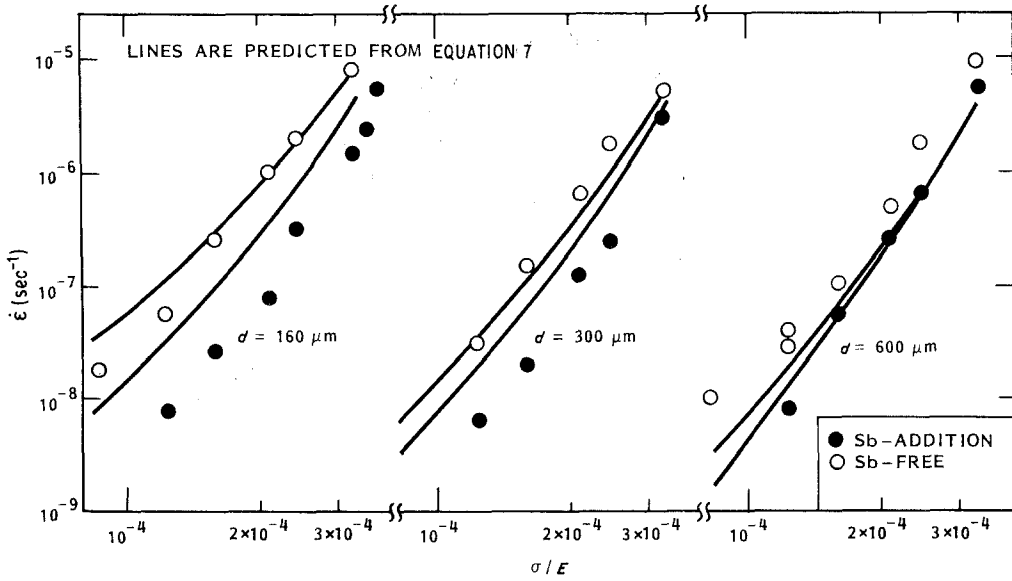


Figure 5 The creep rate–stress behaviour is shown at 1173 K for the 25Cr–20Ni stainless steel in the gbs and slip creep regime at high stresses and coarse grain sizes.

the creep rate can be written as:

$$\dot{\epsilon} = \dot{\epsilon}_{\text{gbs}} + \dot{\epsilon}_{\text{slip}} = A_{\text{gbs}} \alpha 50 \frac{D_p}{d^2} \left(\frac{\sigma}{E} \right)^4 + A_{\text{slip}} \frac{D_L}{b^2} \left(\frac{\sigma}{E} \right)^5 \quad (4)$$

The activation energy for creep as a function of grain size can be calculated from Equation 4 since differentiation of Equation 4 with respect to temperature yields

$$Q_c \Big|_{\sigma/E} = -R \frac{d \ln \dot{\epsilon}}{d(1/T)} \Big|_{\sigma/E} = \left\{ \frac{[(A_{\text{gbs}} \alpha 50) D_p Q_p / d^2] + [A_{\text{slip}} (D_L Q_L / b^2) (\sigma/E)]}{[(A_{\text{gbs}} \alpha 50) D_p / d^2] + [A_{\text{slip}} (D_L / b^2) (\sigma/E)]} \right\} \quad (5)$$

A quantitative prediction can be made using Equation 5 for the change in activation energy for creep with grain size. In order to compare the predicted curve with the experimental data of Fig. 4, it was decided to plot the ratio Q_c/Q_L , rather than Q_L , as a function of grain size. This is because, as explained in the footnote, the absolute values of Q_c obtained by Yamane *et al.* are higher than the normally expected values of Q_p and Q_c for stainless steel. The relation for Q_c/Q_L , rewritten from Equation 5, is:

$$\frac{Q_c}{Q_L} = \frac{B(Q_p/Q_L)(b/d)^2 + 1}{B(b/d)^2 + 1} \quad (6)$$

where

$$B = \left[\left(\frac{A_{\text{gbs}} \alpha 50}{A_{\text{slip}}} \right) \left(\frac{D_p}{D_L} \right) \left(\frac{\sigma}{E} \right)^{-1} \right]$$

Substituting the appropriate values of the various constants to solve for B (Table II and Fig. 4), the predicted relation between Q_c/Q_L and d is readily quantified. The resulting predictions are shown by the full curves in Fig. 4 for the antimony-addition and antimony-free stainless steels. The predicted curves reveal that there is a transition from creep controlled by D_p to D_L at a grain size of about 200 μm for the antimony-addition stainless steel and at a grain size of about 400 μm for the antimony-free stainless steel. The experimentally observed Q_c-d data show a similar pattern for the two stainless steels. The grain sizes at which a transition occurs from a low Q_c to a high Q_c , however, are at lower values (90 to 120 μm) than those predicted (200 to 400 μm). Nevertheless, the fact that the predicted curves show the correct trend of an increase in Q_c with an increase in grain size is another indication that the proposed mechanism of gbs controlled by D_p at fine grain sizes is probably a correct one.

The creep data of Figs. 2 and 3 represent work by Yamane *et al.* [5] for grain sizes from 30 to 160 μm . Yamane *et al.* also investigated coarse grain sizes from 160 to 600 μm . The data for this part of their study are shown in Fig. 5.

The conditions of grain size and creep stress here indicate that these data are represented in the upper region of the Yamane *et al.* study given in the deformation map of Fig. 1. Data in this region can be analysed by a $D_L + D_p$ controlled gbs relation and a $D_L + D_p$ controlled slip creep relation, as shown in the following equation.

$$\dot{\epsilon} = \dot{\epsilon}_{\text{gbs}} + \dot{\epsilon}_{\text{slip}} = A_{\text{gbs}} \frac{D_{\text{eff}}}{d^2} \left(\frac{\sigma}{E} \right)^2 + A_{\text{slip}} \frac{D_{\text{eff}}}{b^2} \left(\frac{\sigma}{E} \right)^5 \quad (7)$$

where

$$D_{\text{eff}} = D_L + \alpha 50 \left(\frac{\sigma}{E} \right)^2 D_p$$

with $\alpha = 4$ for the gbs mechanism and $\alpha = 1$ for the slip creep mechanism. The curves predicted from Equation 7 are given by the full curves in Fig. 5. The experimental data of Yamane *et al.* are given for the three coarsest grain sizes studied (160, 300 and 600 μm). The predictive aspects of the constitutive equations are well illustrated by the convergence of the two curves with an increase in stress or with an increase in grain size. This is a reflection of the dominating influence of subgrains [27] in determining the flow stress in the slip creep region with antimony additions playing an insignificant role.

4. Discussion of correlations

Figs. 2 to 5 convincingly demonstrate that much of the creep data presented by Yamane *et al.* on 25Cr–20Ni stainless steel can be predicted quantitatively when a grain boundary sliding relation involving D_L and D_p is introduced. The “core-and-mantle” model of Gifkins [11] is a very functional model for interpreting the results obtained by Yamane *et al.* The use of different values of the constant A for the gbs relation (Equation 2) for stainless steel with and without antimony reflect the importance of grain boundary segregants in influencing the creep behaviour in the mantle region when grain boundary sliding is important. It is certainly reasonable to expect that the type and nature of the segregant would influence the value of the constant A in the gbs relation given by Equation 2. The specific values of A selected for the two stainless steels reflect well the correct separation of the two stainless steels in both σ^2 and σ^4 stress

regimes (Fig. 2). On the other hand, grain boundary segregants would not be expected to influence slip creep. In this case deformation occurs principally in the core region of each grain. Thus, similar creep behaviour is observed in the two stainless steels at coarse grain sizes (Fig. 5). Similarly, α in the term $\alpha f_p D_p$ of Equation 3 is also a variable to consider in creep deformation by gbs and by slip creep. The $\alpha f_p D_p$ term reflects the contribution of the dislocation structure, in the core and mantle regions, to the creep rate. The value of α is considered equal to 1 in slip creep where the core of the grain plays the major role in deformation [12, 23, 32]. The value of α was chosen equal to 4 in this study, in order to fit the gbs relation to the stainless steel data (Fig. 2). This value of α relates to the dislocation structure contribution to creep in the mantle region of each grain. A value of α larger than 1 would imply that the dislocation density is higher in the mantle region than in the core region. This is in agreement with experimental observations [35, 36]. Use of the relation $\alpha f_p D_p$ permits prediction of several regions in the Yamane *et al.* [5] data: (1) The stress dependence of creep goes from a second-order power-law behaviour to a fourth-order power-law behaviour for the 25Cr–20Ni stainless steel (Fig. 2) with the same grain size dependence in both stress regions (Fig. 3). (2) Evidence for D_p controlling gbs, combined with the additive contribution of slip creep, is also seen in the activation energy variation with grain size (Fig. 4) and in the stress dependence of the creep rate at high stresses (Fig. 5).

No threshold stress is evident using the approach taken in this paper, nor it is necessary to incorporate one to describe the data. Yamane *et al.* analysed their data with a diffusional creep relation involving a threshold stress. No threshold stress is expected in stainless steel, however, because there is no convincing experimental evidence for such a stress in single-phase metallic materials. Thus, even though a threshold stress may exist for diffusional flow or grain boundary sliding, no threshold stress would be expected for such materials when slip creep is the rate-controlling mechanism. With these considerations as a basis, Fig. 6 was constructed to illustrate the predicted creep behaviour of a polycrystalline 25Cr–20Ni stainless steel at $0.7T_m$. The creep rate–flow stress relation is

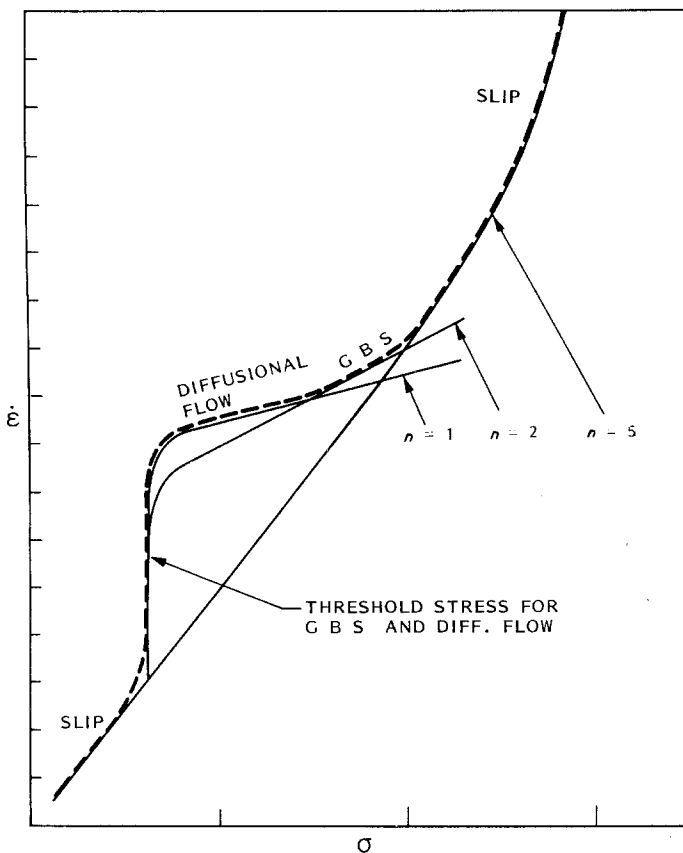


Figure 6 An overview of the predicted creep behaviour of a polycrystalline 25Cr-20Ni stainless steel at $0.7T_m$ incorporating slip creep, grain boundary sliding and diffusional mechanisms of creep. The broken curve on the $\log \dot{\epsilon}$ against $\log \sigma$ plot shows the overall behaviour of the steel.

depicted for all three deformation mechanisms: slip creep, grain boundary sliding and diffusional creep. A threshold stress is shown to exist for grain boundary sliding and diffusional creep, of a magnitude which was, for convenience, made the same for both mechanisms. No threshold stress is shown for the slip creep mechanism since no evidence appears to exist for such a threshold in massive single-phase materials. The broken curve shown in Fig. 6 shows the predicted creep rate-stress relation over a wide range of stress. As can be seen, slip creep dominates the deformation process both at high stresses and at low stresses. At intermediate stresses, gbs and diffusional creep intervene as faster processes than slip creep. The threshold stress enters to inhibit gbs and diffusional creep at low stresses and thus allows slip to become the rate-controlling process again.

Yamane *et al.* [5] interpreted their data for the antimony-free stainless steel at low stresses to follow a one-power-law behaviour (Fig. 2). This region of low slope was identified by Yamane *et al.* as due to diffusional (Coble) creep. The major argument against this conclu-

sion is that the actual creep rates are considerably faster than those predicted by the Coble relation (see Figs. 2 and 3). For this reason, we consider that the most likely mechanism taking place is gbs rather than diffusional creep. Only at stresses considerably below $\sigma = 10^{-5}E$ can diffusional flow be expected to be rate-controlling.

5. Conclusions

Grain boundary sliding (gbs) is an important mechanism of plastic flow in fine-grain austenitic stainless steels at high homologous temperatures. A phenomenological equation developed to describe gbs and superplastic flow correctly predicts a strong grain size dependence ($\dot{\epsilon} \propto d^{-2}$) in the stress range where the creep rate is proportional to the second and to the fourth power of stress. Deformation by diffusional flow mechanisms will only become important when very low stresses, e.g. $\sigma \leq 10^{-5}E$, are achieved. No threshold stress for creep is observed, nor expected, in the creep of austenitic stainless steel when gbs and slip mechanisms are taken into account.

Acknowledgements

Support of this investigation is through the US Office of Naval Research under Contract N-00014-82-K-0314. The authors are pleased to acknowledge encouragement and guidance from Dr Bruce MacDonald.

References

1. Y. TAKAHASHI, K. NAKAGAWA and T. YAMANE, *Z. Metallkde.* **71** (1980)
2. Y. TAKAHASHI and T. YAMANE, *J. Mater. Sci.* **16** (1981) 3171.
3. *Idem*, *ibid.* **16** (1981) 3171.
4. *Idem*, *Scripta Metall.* **16** (1982) 1137.
5. T. YAMANE, N. GENMA and Y. TAKAHASHI, *J. Mater. Sci.* **19** (1984) 263.
6. O. D. SHERBY and O. A. RUANO, "Superplastic Forming of Structural Alloys", edited by N. C. Paton and C. H. Hamilton (TMS-AIME, New York, 1982) p. 241.
7. J. WADSWORTH and O. D. SHERBY, "Deformation Processing and Structure", edited by G. Krauss (ASM, Metals Park, Ohio, 1984) Ch. 8, p. 355.
8. A. BALL and M. M. HUTCHINSON, *Met. Sci. J.* **3** (1969) 1.
9. T. G. LANGDON, *Phil. Mag.* **22** (1970) 689.
10. A. K. MUKHERJEE, *Mater. Sci. Eng.* **8** (1971) 83.
11. R. C. GIFKINS, *Metall. Trans.* **7A** (1976) 1225.
12. M. F. ASHBY and H. J. FROST, in "Constitutive Equations in Plasticity", edited by A. J. Argon (MIT, Cambridge, MA, 1975) p. 117.
13. F. A. MOHAMED and T. F. LANGDON, *Metall. Trans.* **5** (1974) 2339.
14. T. G. LANGDON and F. A. MOHAMED, *Mater. Sci. Eng.* **32** (1978) 103.
15. O. A. RUANO and O. D. SHERBY, *ibid.* **56** (1982) 167.
16. B. WALSER and O. D. SHERBY, *Scripta Metall.* **16** (1982) 213.
17. F. R. N. NABARRO, Report of the Conference on the Strength of Solids (Physical Society, London, 1948) p. 75.
18. C. HERRING, *J. Appl. Phys.* **21** (1950) 437.
19. R. L. COBLE, *ibid.* **34** (1963) 1679.
20. H. LUTHY, R. A. WHITE and O. D. SHERBY, *Mater. Sci. Eng.* **39** (1979) 211.
21. O. A. RUANO and O. D. SHERBY, *ibid.* **51** (1981) 9.
22. J. HARPER and J. E. DORN, *Acta Metall.* **5** (1957) 564.
23. S. L. ROBINSON and O. D. SHERBY, *ibid.* **17** (1969) 109.
24. R. A. WHITE, PhD Dissertation, Stanford University, California (1978).
25. F. GAROFALO, W. F. DOMIS and F. VON GEMMINGEN, *Trans AIME* **230** (1964) 1460.
26. T. SRITHARAN and H. JONES, *Acta Metall.* **28** (1980) 1633.
27. O. D. SHERBY and P. M. BURKE, *Prog. Mater. Sci.* **13** (1967) 333.
28. C. LEYMONIE, Y. ADDA, A. KIRIANENKO and P. LACOMBE, *C.R. Acad. Sci. Paris* **248** (1959) 1512.
29. D. W. JAMES and G. A. LEAK, *Phil. Mag.* **12** (1965) 491.
30. P. LACOMBE, P. GUIRALDENG and C. LEYMONIE, "Radioisotopes in the Physical Science Industry" (IAEA, Vienna, 1962) p. 179.
31. W. KOSTER, *Z. Metallkde.* **39** (1948) 1.
32. H. LUTHY, A. K. MILLER and O. D. SHERBY, *Acta Metall.* **28** (1980) 169.
33. C. G. SCHMIDT and A. K. MILLER, *ibid.* **30** (1982) 614.
34. P. C. J. GALLAGHER, *Metall. Trans.* **1** (1970) 2429.
35. J. L. LYTTON, C. R. BARRETT and O. D. SHERBY, *Trans. AIME* **233** (1965) 1399.
36. M. C. MATAYA, M. J. CARR and G. KRAUSS, *Metall. Trans.* **15A** (1984) 347.

Received 13 November
and accepted 28 November